Frontiers of Information Technology & Electronic Engineering
www.jzus.zju.edu.cn; engineering.cae.cn; www.springerlink.com
ISSN 2095-9184 (print); ISSN 2095-9230 (online)
E-mail: jzus@zju.edu.cn

# Interpreting the vulnerability of power systems in cascading failures using multi-graph convolutional networks*

Supaporn LONAPALAWONG[1], Changsheng CHEN[2], Can WANG[3], Wei CHEN‡[1]

[1]*State Key Lab of CAD & CG, Zhejiang University, Hangzhou 310058, China*

[2]*China Electric Power Research Institute, Beijing 100192, China*

[3]*College of Computer Science and Technology, Zhejiang University, Hangzhou 310058, China*

E-mail: 11821132@zju.edu.cn; ccs9032@163.com; wcan@zju.edu.cn; chenwei@cad.zju.edu.cn

Received Jan. 27, 2022; Revision accepted Mar. 24, 2022; Crosschecked Apr. 24, 2022; Published online June 20, 2022

**Abstract:** Analyzing the vulnerability of power systems in cascading failures is generally regarded as a challenging problem. Although existing studies can extract some critical rules, they fail to capture the complex subtleties under different operational conditions. In recent years, several deep learning methods have been applied to address this issue. However, most of the existing deep learning methods consider only the grid topology of a power system in terms of topological connections, but do not encompass a power system's spatial information such as the electrical distance to increase the accuracy in the process of graph convolution. In this paper, we construct a novel power-weighted line graph that uses power system topology and spatial information to optimize the edge weight assignment of the line graph. Then we propose a multi-graph convolutional network (MGCN) based on a graph classification task, which preserves a power system's spatial correlations and captures the relationships among physical components. Our model can better handle the problem with power systems that have parallel lines, where our method can maintain desirable accuracy in modeling systems with these extra topology features. To increase the interpretability of the model, we present the MGCN using layer-wise relevance propagation and quantify the contributing factors of model classification.

**Key words:** Power systems; Vulnerability; Cascading failures; Multi-graph convolutional networks; Weighted line graph

https://doi.org/10.1631/FITEE.2200035 **CLC number:** TP393

## 1 Introduction

The power system is one of the critical infrastructures that support the overall efficiency of people's daily lives. In March 2019, fires in local vegetation and cyberattacks caused more than 20 hours of power outage, with a massive blackout that left more than 70% of Venezuelans without electricity. The blackout caused a massive disruption to the public transportation services in the capital of Caracas, where gas stations shut down and could not distribute fuel during the power outage, and the blackout even disrupted the operations of the local hospital. These catastrophic failure cascades pose a significant threat to human life and national security. Thus, it is important to understand and examine the vulnerability of power systems in cascading failures (Chen G et al., 2010; Zhang and Tse, 2015; Gambuzza et al., 2017).

Analyzing the vulnerability of power systems in a cascading failure event has been the focus of many researchers in recent years (Zhu et al., 2014; Fang et al., 2021). Many researchers have explored

‡ Corresponding author

* Project supported by the National Natural Science Foundation of China (No. U1866602) and the Natural Science Foundation of Zhejiang Province, China (No. LZ22F020015)

ORCID: Supaporn LONAPALAWONG, https://orcid.org/0000-0002-4032-7740; Changsheng CHEN, https://orcid.org/0000-0001-9128-4165; Wei CHEN, https://orcid.org/0000-0002-9853-8049

models and methods using structural vulnerability analysis and functional shortcoming analysis. Structural vulnerability analysis focuses mainly on topological weaknesses, abstracts power systems as complex networks, and studies the relationship between the topology and physical behavior of power systems (Schneider et al., 2011; Wu et al., 2011; Ren et al., 2018; Lonapalawong et al., 2022). Functional shortcoming analysis considers a more detailed dynamic cascading failure process by incorporating the underlying physical techniques and high-level network-based models (Mei et al., 2009; Eppstein and Hines, 2012; Zhang et al., 2017). Although several studies have been devoted to analyzing power grid vulnerability, they failed to capture the complex subtleties under different operational conditions (e.g., load patterns and branch flow patterns). As a result, the topologies, capacity settings, and other parameters often produce inconsistent or even contradictory results in regard to the effects of failures. To better understand power system vulnerability, the models used for analysis need to focus on the relevant features in data.

With the rise of artificial intelligence (AI) technologies, a technique using the data-driven fault detection and classification method shows improved performance over previous approaches. Deep learning is a type of machine learning and AI that imitates the way humans gain certain types of knowledge, with the model having no need to understand the features that the data represent. Deep learning has been applied to various areas of the power system, such as fault diagnosis (Luo et al., 2019; Chen KJ et al., 2020), cascading failure search (Liu et al., 2021), scenario generation (Ge et al., 2020), optimal load shedding (Kim et al., 2019), and power outage forecasting (Owerko et al., 2018). The graph convolutional network (GCN) is a deep learning based method that operates in the graph domain. GCNs are a powerful type of neural network designed to work directly on graphs and leverage their structural information.

Although GCNs have strong ability for feature extraction and can capture the topological components, using this method to consider the properties of the power system still requires further research. Three critical problems remain to be addressed to build better deep learning models. First, the simple graph connection representation in GCN graph input (0: disconnected, 1: connected) is not sufficiently effective in capturing the power system's spatial information. Second, a common assumption of a GCN is that there is at most one edge between any pair of nodes. Due to the complexity of power systems, nodes have a variety of relationships with different semantic, physical, or abstract meanings, e.g., the connection of a generator to a consumer or a consumer to a consumer. Finally, GCNs are seen as "black-box" models, which makes it difficult to explain how and why the system reaches a particular outcome.

In this study, we focus on power system vulnerability, viewed as a graph in a cascading failure, based on the branch information. Special graph structures (such as line graphs) improve messaging operations in neural graph networks from different graph perspectives. To better understand the information from the branch relationship perspective, we convert the power system topology to a line graph topology and consider the spatial information that describes the informative edge by adjusting weight importance. Then we propose a multi-graph convolutional network (MGCN) model to classify the power system's vulnerability level in a cascading failure. Unlike existing deep learning models, our model supports the concept of multi-graphs, which has multiple edges. The proposed model's architecture preserves the power system's spatial correlations and the model is designed to exploit the line graph concept for edge representation by converting the given power system to a weighted line graph. To increase the interpretability of the model, we explain the MGCN model using a layer-wise relevance propagation (LRP) algorithm (Montavon et al., 2019; Kohlbrenner et al., 2020) and quantify the model prediction contributing factors. From the given data, LRP produces patterns that identify evidence for or against a prediction target. Furthermore, experimental results on four real-world datasets demonstrate that our model can effectively capture the topology and feature correlations from the power system and that our power-weighted line graph based MGCN model outperforms various existing methods. The contributions of this study are as follows:

1. We propose an MGCN model to learn the graph features while considering the power system topology information with a variable graph structure and size.

2. Using the edge representation in the graph, a more informative representation of the power system as a weighted line graph is presented.

3. The LRP model is applied to identify the contributing factors that may have caused the cascading failures and to manage the power system to mitigate the damage.

## 2 Related works

Our work is related to analyzing power system vulnerability in cascading failures using GCNs in the power system, and to the interpretation of graph neural networks (GNNs). Here, we briefly review the related works in these fields of research.

### 2.1 Analyzing power system vulnerability in cascading failures

A critical subject in power system vulnerability analysis is identifying the essential components in a power system. Various exogenous contingencies usually initiate cascading failures, such as natural disasters and intentional attacks (Zhu et al., 2014; Fang et al., 2021). The existing works can be divided into two basic categories: structural vulnerability analysis and functional shortcoming analysis. Structural vulnerability analysis focuses mainly on the structural changes of the system by comparing the number of nodes and links of the residual network after the cascading failure process with that of the original network (Schneider et al., 2011; Wu et al., 2011; Ren et al., 2018; Lonapalawong et al., 2022). Pizzuti et al. (2020) investigated the role of the effective resistance matrix and the link-betweenness strategies to identify the links causing severe damages to the network. Ren et al. (2018) introduced a stochastic model to study the dynamics of cascading failure evolution in a Barabási–Albert scale-free network. Such analytical indices provide efficient vulnerability analysis, but they cannot sufficiently capture the islanding or re-dispatching events in the whole cascading failure procedure. Lonapalawong et al. (2022) proposed a topology-based greedy strategy to optimize the robustness of the power system and to measure the optimal topology using average propagation. The functional methods consider a more detailed dynamic process by incorporating the underlying physical techniques and high-level network-based models (Mei et al., 2009; Eppstein and Hines, 2012; Zhang et al., 2017). di Muro et al. (2017) applied the concepts of internal and external functionality rules for intra- and inter-network dependencies to analyze different conditions of internal node failures due to disconnection from nodes within the power grid's network. Song et al. (2016) described the cascading outage simulator with multiprocess integration capabilities (COSMIC), a new non-linear dynamic model, using a recursive process to compute the impact of the triggering event(s). Some researchers studied both the topological features and the effect of flow dynamics on network robustness in cascading failures. Li X and Qi (2021) proposed a new method to identify the vulnerable lines in power systems and to predict the cascading failure path based on the line degree and line overload risk.

Our work analyzes power system vulnerability by simulating the dataset based on functional methods and combining the structure topology to predict the component outage level in cascading failures.

### 2.2 Using graph convolutional networks in power systems

GCNs can be expanded from convolutional neural networks (CNNs) to handle arbitrary graph-structured data. This approach has recently received widespread attention. Bruna et al. (2014) first introduced GCN, in which convolutional layers were applied to graph data. In Kipf and Welling (2017), a novel CNN variant was proposed which can be used directly on graphs, and the network performed well on tasks involving graph node classification. In addition to semi-supervised classification (Kipf and Welling, 2017), system recommendation (Ying et al., 2018), and traffic prediction, GCN has been successfully used in many applications. With respect to power systems, Chen KJ et al. (2020) developed a GCN framework for the positioning of faults in power distribution networks. Liao et al. (2021) designed a GCN for transformer fault diagnosis. Owerko et al. (2018) applied GCNs to adequately process weather measurements to determine the likelihood of a power outage. Liu et al. (2021) used GCNs to identify critical cascading failure paths that result in load shedding. Bolz et al. (2019) applied GCNs to approximate alternating current (AC) power flow in power systems. Kim et al. (2019) considered the optimal power flow, which is a different calculation type from

the load flow, without weight sharing that usually obstructs a reasonable extrapolation of patterns.

We focus on multi-graphs, in which each graph is permitted to have multiple edges between a pair of nodes. One single relation type may not describe relationships comprehensively; we construct multiple graphs and further design an MGCN to capture the relationships among different semantic, physical, or abstract meanings.

### 2.3 Interpretation of graph neural networks

Deep neural networks (DNNs) are good for learning complex networks and gaining powerful representations, but they are often considered to be "black-boxes." To better understand classifier decisions and gain insight into how these models operate, various techniques have been proposed (Zeiler and Fergus, 2014; Springenberg et al., 2015; Zhou et al., 2016). All these works provide insights for understanding and improving the neural network models. To determine how the prediction values are generated from the original input values, LRP was introduced in Bach et al. (2015), which explained how input data support the prediction in the trained model.

An LRP algorithm explains a classifier's prediction specific to a given data point by attributing relevance scores to essential components of the input using the topology of the learned model itself (Montavon et al., 2019). Schnake et al. (2020) explained neural networks by finding a scoring of walks in the graph instead of individual nodes or edges. Hu et al. (2020) proposed a new LRP algorithm that explains a GCN method.

## 3 Proposed method

In this section, we separate the model into two parts: data construction and an MGCN model.

### 3.1 Data construction

#### 3.1.1 Cascading failure simulation

According to the actual operation of power systems in recent years, a cascading failure is a threat to power systems' safe and reliable operation. $N-1$ contingency is a common method in power grid reliability analysis (Zhang et al., 2017). The ORNL-PSERC-Alaska (OPA) model has been widely adopted (Zhu et al., 2014; Fang et al., 2021). The model contains two layers of iterations. The inner iteration is concerned with the fast dynamics, which simulates the power flow, while the outer iteration focuses on slow dynamics, which simulates the growth of the power grid (such as the increase of generation and load and the update of transmission lines). In this study, we consider only the inner iteration.

Fig. 1 illustrates the inner iteration of the improved OPA model. Compared to the original OPA model, the two shadow blocks show differences. The improved OPA model considers the dispatching center's failure due to some contingencies (shadow diamond), such as communication interruption. In the shadow rectangle, part I represents the method of tripping overload lines, which is used by both the original and improved OPA models; i.e., the lines with power flows that exceed a certain proportion of the limits are assumed to be overloaded lines and are tripped with a probability $\beta$. Part II is employed only by an improved OPA model representing the tripping of normal lines caused by hidden failures. $\xi$ is the base probability of unwanted relay protection operations.

After finishing the simulation, we obtain the structure and features of a cascading failure sample.

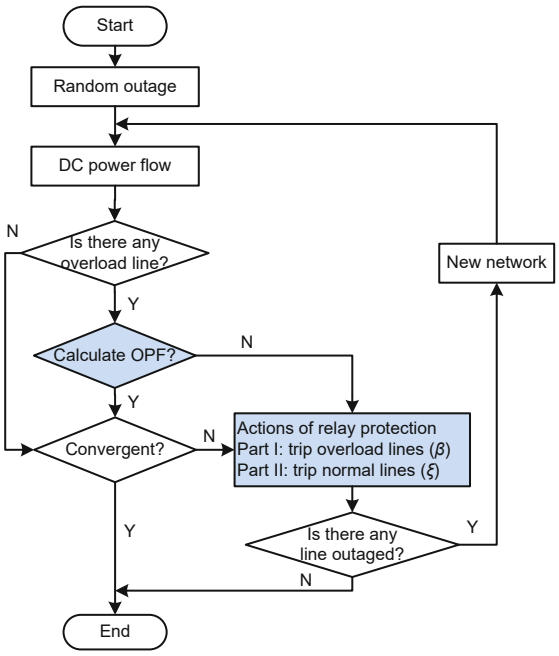


**Fig. 1 Inner iteration of the improved ORNL-PSERC-Alaska (OPA) model (DC: direct current; OPF: optimal power flow)**

Every sample includes five elements, the topological connection, branch flow, busload, protection relay, and component outage, as part of the GCN. The component outage as a target class of this work is divided into three categories: low, medium, and high levels of the overall line tripped in each case. All of the feature information comes from the suggestions of an expert.

### 3.1.2 Line graph transformation

GNNs capture interactions between nodes by transferring messages between them; however, this study focuses on the branch triggering in a cascading failure. The branches of the power system are represented by the features generated by the OPA model in Section 3.1.1. As a result, we create a line graph that converts the branches to nodes. When the two branches in the power network domain have ordinary buses, the two nodes in the graph domain are connected. Consider an undirected graph $G=(N,E)$, where $N$ is the node set and $E$ is the edge set with unordered pairs of elements in $N$. The line graph $L(G)$ is a graph in which each node is an edge in $G$, and two nodes are neighbors if and only if their corresponding edges in $G$ share a common terminal vertex. The conversion to a line graph is shown in Fig. 2. As a result, the simple line graph is insufficient to encompass all power system information, officially $L(G)=(N_{\mathrm{L}},E_{\mathrm{L}})$, where $N_{\mathrm{L}}=\{(n_u,n_v):(n_u,n_v)\in E\}$ and $E_{\mathrm{L}}=\{((n_u,n_v),(n_v,n_w)):(n_u,n_v)\in E,(n_v,n_w)\in E\}$.

It is important to note, however, that not all network edges are equally significant. For example, a social network can connect millions of fans to a movie star, but no two fans may be alike. Due to this, the relationship between one fan and the movie star (weight of the corresponding edge) may be weaker than that between another fan and the movie star. Additionally, the embeddings of lines that are similar in topography or semantics should be comparable.

### 3.1.3 Weighted line graph

Inspired by Bandyopadhyay et al. (2019), we develop graph representation algorithms for directly embedding edges in an information network. Bandyopadhyay et al. (2019) showed that using graphs in this way could represent a basis for solving some of the issues in the context of network embedding and help move network representation learning beyond node embedding.

In $L(G)$, the topology information of the original graph $G$ is encoded, but its dynamics and topology are not properly represented. Each edge's attributes include those of its two end nodes. A vertex with a degree $d$ in the original graph $G$ will have $d(d-1)/2$ edges in the line graph $L(G)$. By contrast, the topology structure of $L(G)$ will overstate the importance of features for nodes with high degrees in the graph, but understate the importance of nodes with a lower degree, which leads to biased topology information being encoded in the line graph. By combining the node degree and edge weight, we construct a new weighted line graph to correct the bias. To facilitate a random walk on $L(G)$, the edge weights are defined. Intuitively, if we start a random walk from node $n_{uv}\equiv(n_u,n_v)\in L(G)$ and want to traverse to $n_{vw}\equiv(n_v,n_w)\in L(G)$, this is equivalent to selecting node $n_v\in G$ from $(n_u,n_v)$ and moving to $n_w\in G$. If $G$ is undirected, we define the probability of choosing $n_v$ to be proportional to $d_{n_u}/(d_{n_u}+d_{n_v})$. Here, $d_{n_u}$ and $d_{n_v}$ are the degrees of the endpoint nodes of edge $(n_u,n_v)$. In general, an

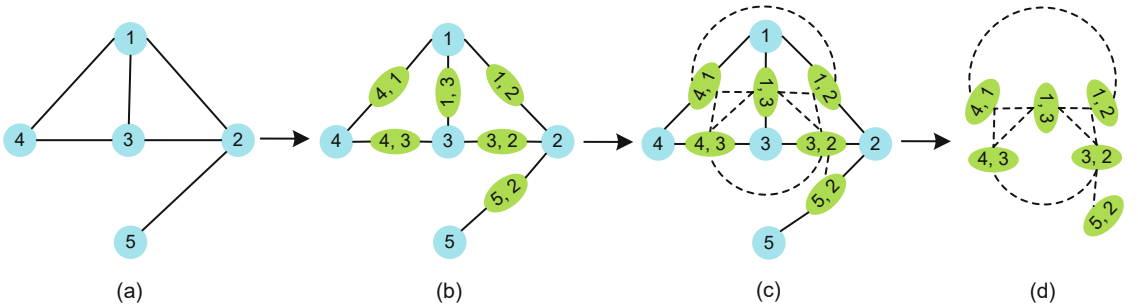


**Fig. 2 Transformation process of a graph into its line graph: (a) graph $G$; (b) nodes in $L(G)$ added; (c) edges in $L(G)$ added; (d) line graph $L(G)$**

edge is more relevant to the endpoint node with the lower degree than to the other endpoint node with the higher degree.

We define the edge weight for edge $(e_{uv}, e_{vw})$ of line graph $L(G)$ as follows:

$$w_{(e_{uv},e_{vw})} = \frac{d_u}{d_u + d_v} \cdot \frac{w_{vw}}{\sum\limits_{r\in\mathcal{N}(v_v)} w_{vr} - w_{uv}}, \quad (1)$$

where $d_u$ and $d_v$ are the degrees of nodes $u$ and $v$ in the original graph $G$ respectively, and $w_{vw}$, $w_{vr}$, and $w_{uv}$ are weights according to the original graph.

#### 3.1.4 Constructing the power system topology

The concept of weighted line graph can capture the edge importance based on the graph structure, but cannot identify the power system's spatial information. In a power system, the electrical impedance $(Z)$ is the total opposition to the alternating current. In other words, the whole thing in the circuit "impedes" the flow of the current. The impedance is measured in Ohms and can include resistance $(R)$, inductive reactance $(X_{\mathrm{L}})$, and capacitive reactance $(X_{\mathrm{C}})$. We can combine resistance and reactance as impedance in a simple vector way (Fig. 3). From this concept, we can identify "electrical distance" as the impedance value, that is, the quantification of the spatial correlation of the power system. The new line weight is as follows:

$$e_{uv} = \begin{cases} \frac{1}{\sqrt{R_{uv}^2 + X_{uv}^2}}, & \text{if nodes } u \text{ and } v \text{ are connected,} \\ 0, & \text{otherwise,} \end{cases} \quad (2)$$

where $R_{uv}$ and $X_{uv}$ respectively represent the line resistance and reactance of bus nodes $u$ and $v$.

A longer distance or a larger impedance indicates a smaller correlation between nodes (Tong et al., 2021).

Finally, we combine Eqs. (1) and (2) as a new weighted adjacency matrix of the input GCN model. Fig. 4 illustrates the IEEE 9-bus system with a different kind of weighted line graph.

### 3.2 Multi-graph convolutional network and interpretation

#### 3.2.1 Multi-graph convolutional network

In a typical power system, we can usually find that large-scale topologies have several lines connected in parallel (Fig. 5). These structures represent a strategy to help prevent widespread blackouts: if the electrical grid has high redundancy, one can disconnect any line without worrying about any other line connected to it, thus ensuring that problems or scheduled maintenance creates blackouts only in small, controlled areas. From this issue, our model focuses on multi-graphs, in which each graph is permitted to have multiple edges. The system architecture of the proposed MGCN model is shown in Fig. 6. As seen on the left side of Fig. 6, the constructed node features (Section 3.1.1) and the power-weighted line graph (Section 3.1.4) are considered as the inputs of the model, and then an MGCN is designed to capture the spatial dependency of the power system.

Compared to non-spectral GCNs, spectral models have filters with more global support, which is important for capturing complex relationships. Spectral GCNs are based on a Laplacian matrix.

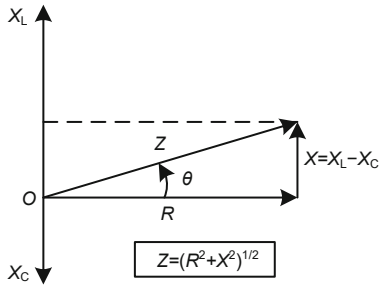


**Fig. 3 Identifying impedance as the electrical distance: impedance ($Z$) is a measure of how much the circuit impedes the charge flow. Impedance can be split into two parts: resistance $R$ (the part that is constant, regardless of frequency) and reactance $X$ (the part that varies with frequency due to capacitance and inductance)**

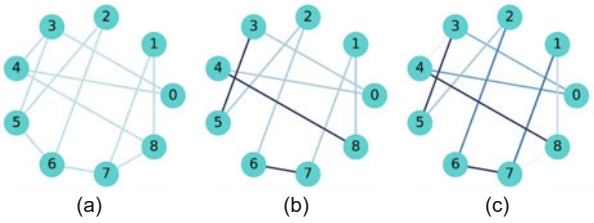


**Fig. 4 IEEE 9-bus system with different weighted line graphs: (a) original line graph; (b) weighted line graph that captures the structural degree; (c) power-weighted line graph that captures both structural degree and electrical distance. An edge with a larger weight is displayed darker. References to color refer to the online version of this figure**

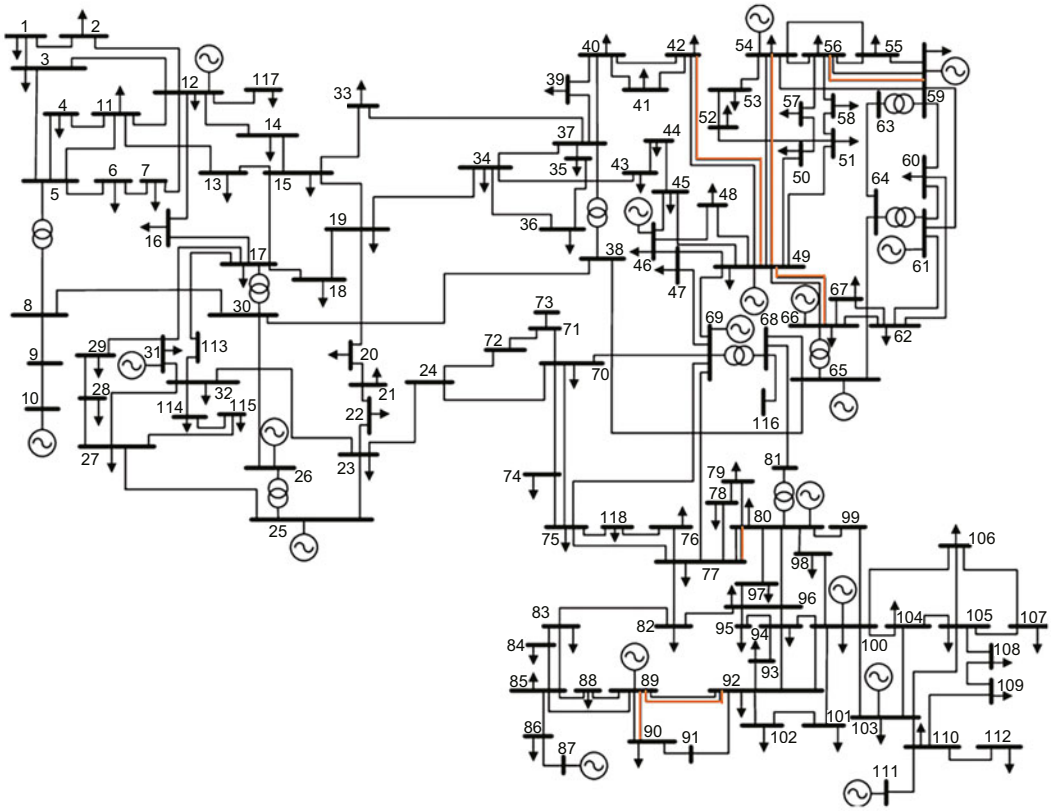

**Fig. 5 Topology of IEEE 118 with parallel (double) lines (orange lines represent the redundancy lines). References to color refer to the online version of this figure**

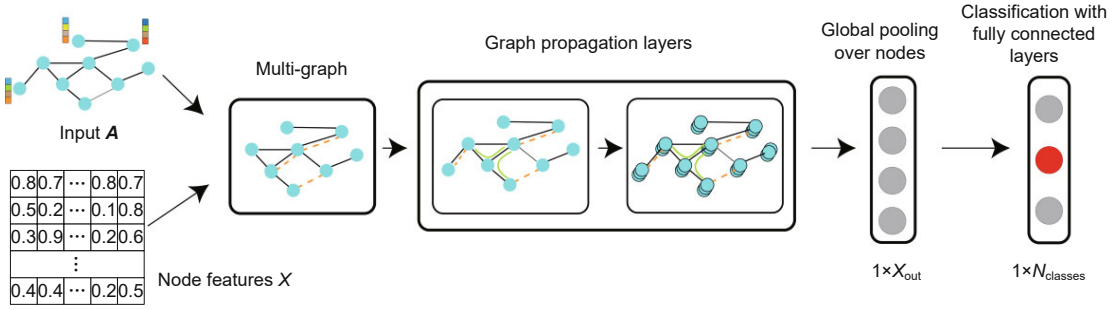


**Fig. 6 Pipeline for graph classification. In our model, the network is sent through the $l^{\text{th}}$ convolutional layer, which produces a graph with identical nodes and edges. As the receptive field grows larger, the node features of our line graph become increasingly global, but the edges remain unchanged. As a consequence, each node in the graph includes information about its neighbors and the complete graph after numerous graph convolutional layers. We summarize the data acquired by each node by pooling it over nodes. To conduct classification, fully connected layers use global pooling. Connections learned as outlined in Eq. (9) are indicated by a dashed orange line. References to color refer to the online version of this figure**

For an undirected graph, suppose $\boldsymbol{A}$ is the adjacency matrix of the graph, and $\boldsymbol{D}$ is a diagonal matrix of node degrees with $D_{ii}=\sigma_j(A_{ij})$. A graph Laplacian matrix is defined as $\boldsymbol{L}=\boldsymbol{D}-\boldsymbol{A}$. A Laplacian matrix's normalized format is defined as $\boldsymbol{L}^{\text{sym}}=\boldsymbol{D}^{-1/2}\boldsymbol{L}\boldsymbol{D}^{-1/2}=\boldsymbol{I}-\boldsymbol{D}^{-1/2}\boldsymbol{A}\boldsymbol{D}^{-1/2}$, which is a matrix representation of a graph that may be used to identify various important features of the graph ($\boldsymbol{I}$ is an identity matrix with appropriate dimensions). $\boldsymbol{L}^{\text{sym}}$ is symmetric and positive-semidefinite. With these properties, the normalized Laplacian matrix $\boldsymbol{L}^{\text{sym}}$ can be factored as $\boldsymbol{L}^{\text{sym}}=\left(\boldsymbol{U}\boldsymbol{\Lambda}\boldsymbol{U}^{\text{T}}\right)^{K}$, where

$\boldsymbol{U} \in \mathbb{R}^{N\times N}$ is the matrix of eigenvectors ordered by eigenvalues, $\boldsymbol{\Lambda}$ is the diagonal matrix of eigenvalues, and $K$ is a Chebyshev filter size.

The spectral convolutions on the graphs are defined as the multiplication of $\boldsymbol{x}$ with a filter $\boldsymbol{g} \in \mathbb{R}^N$ in the Fourier domain by applying the convolution theorem to the graph Fourier transform:

$$\boldsymbol{x} * \boldsymbol{g} = F^{-1}\left(F(\boldsymbol{x}) \odot F(\boldsymbol{g})\right) = \boldsymbol{U}\left(\boldsymbol{U}^{\mathrm{T}}\boldsymbol{x} \odot \boldsymbol{U}^{\mathrm{T}}\boldsymbol{g}\right), \tag{3}$$

where $\boldsymbol{x} \in \mathbb{R}^N$ is the feature vector of the graph's nodes, "$*$" represents the convolution operation, and "$\odot$" represents the Hadamard product. By defining filter $\boldsymbol{g}$ as $\boldsymbol{g}_\theta = \mathrm{diag}\left(\boldsymbol{U}^{\mathrm{T}}\boldsymbol{g}\right)$, Eq. (3) can be simplified as

$$\boldsymbol{x} * \boldsymbol{g}_\theta = \boldsymbol{U}\boldsymbol{g}_\theta\boldsymbol{U}^{\mathrm{T}}\boldsymbol{x}. \tag{4}$$

Here, we can understand $\boldsymbol{g}_\theta$ as a function of the eigenvalues of $\boldsymbol{L}^{\mathrm{sym}}$, i.e., $\boldsymbol{g}_\theta(\boldsymbol{\Lambda})$.

Kipf and Welling (2017) proposed a first-order approximation of ChebNet, assuming $K = 1$ and $\lambda_{\max} = 2$ to obtain a linear function. The convolution of signal $\boldsymbol{x}$ with filter $\boldsymbol{g}_\theta$ in Eq. (4) simplifies to

$$\boldsymbol{x} * \boldsymbol{g}_\theta = \boldsymbol{\theta}_0\boldsymbol{x} - \boldsymbol{\theta}_1\boldsymbol{D}^{-1/2}\boldsymbol{A}\boldsymbol{D}^{-1/2}\boldsymbol{x}, \tag{5}$$

where $\boldsymbol{\theta}_0$ and $\boldsymbol{\theta}_1$ are parameters.

Furthermore, assuming $\boldsymbol{\theta} = \boldsymbol{\theta}_0 = -\boldsymbol{\theta}_1$, the definition of the graph convolution becomes

$$\boldsymbol{x} * \boldsymbol{g}_\theta = \boldsymbol{\theta}\left(\boldsymbol{I}_N + \boldsymbol{D}^{-1/2}\boldsymbol{A}\boldsymbol{D}^{-1/2}\right)\boldsymbol{x}. \tag{6}$$

Finally, we can generalize this definition of the graph convolutional layer:

$$\boldsymbol{Z} = \tilde{\boldsymbol{D}}^{-1/2}\tilde{\boldsymbol{A}}\tilde{\boldsymbol{D}}^{-1/2}\boldsymbol{X}\boldsymbol{\Theta}, \tag{7}$$

where a variable with "$\sim$" means that normalization has been done.

In the approximate spectral graph convolution, the graph Laplacian encodes a single relation type between nodes, extending Eq. (7) to a multi-graph, i.e., a graph with multiple ($R \geq 1$) edges (relations) between the same nodes encoded as a set of graph Laplacians $\{\tilde{L}^{(r)}\}_1^R$, where $R$ is an upper bound on the number of edges per dyad. We straightforwardly concatenate features $\bar{X}^{(r)}$ for all $R$ relation types and learn a single matrix of weights $\boldsymbol{\Theta} \in \mathbb{R}^{(X_{\mathrm{in}}KR)\times X_{\mathrm{out}}}$ :

$$\boldsymbol{Z} = \tilde{\boldsymbol{D}}^{-1/2}\tilde{\boldsymbol{A}}\tilde{\boldsymbol{D}}^{-1/2}\left[\bar{X}^{(0)}, \bar{X}^{(1)}, \ldots, \bar{X}^{(R-1)}\right]\boldsymbol{\Theta}. \tag{8}$$

To study the multi-graph, we devise abstract learning edges jointly with a GCN (Knyazev et al., 2018). We propose to learn a new edge $e_{uv}^{(r)}$ between any pair of nodes $n_u$ and $n_v$ with features $X_u$ and $X_v$ using a trainable similarity function:

$$e_{uv}^{(r)} = \frac{\exp\left(f_{\mathrm{edge}}\ (X_u, X_v)\right)}{\sum_{w=1}^{|N|}\exp\left(f_{\mathrm{edge}}\ (X_u, X_w)\right)}, \tag{9}$$

where $|N|$ denotes the number of nodes in $N$, the softmax function is used to enforce sparse connections, and $f_{\mathrm{edge}}$ can be any differentiable function such as a multi-layer perceptron in our work. This idea is similar to that in Henaff et al. (2015), built on the early spectral convolutional model (Bruna et al., 2014), which learns an adjacency matrix, but with targeted classification tasks for non-graph-structured data.

To simplify the model while maintaining classification accuracy, we exclude pooling layers between convolutional layers and perform maximum global pooling over nodes following the last convolutional layer.

### 3.2.2 Interpretation of GCN

To understand the model prediction, we implement the LRP algorithm proposed in Montavon et al. (2019). The core idea underlying the LRP algorithm for attributing relevance to individual input nodes is to trace contributions back to the final output node layer by layer. Let $v$ and $w$ be neurons at two consecutive layers of the neural network. Propagating relevance scores $(R_w)_w$ at a given layer (i.e., the $w^{\mathrm{th}}$ later, corresponding to neuron $w$) onto neurons of the lower layer is achieved by applying the rule

$$R_v = \sum_w \frac{z_{vw}}{\sum_j z_{vw}} R_w, \tag{10}$$

where $z_{vw}$ models the extent to which neuron $v$ has contributed to make neuron $w$ relevant. The propagation procedure terminates once the input features have been reached. Using the rule above for all neurons in the network, it is easy to verify the layer-wise conservation property $\sum_v R_v = \sum_w R_w$, and by extension, the global conservation property $\sum_u R_u = f(\boldsymbol{x})$.

There are different ways in which the relevance can be distributed over the input node $u$, and different rules for distributing the relevance have been

proposed. In this study, we use the LRP-$\alpha\beta$ rule (as described in Bach et al. (2015)):

$$R_v = \sum_w \left( \alpha \frac{(a_v w_{vw})^+}{\sum_0^v (a_v w_{vw})^+} - \beta \frac{(a_v w_{vw})^-}{\sum_0^v (a_v w_{vw})^-} \right) R_w. \tag{11}$$

Here, we use the notations $(\cdot)^+ = \max(0, \cdot)$ and $(\cdot)^- = \min(0, \cdot)$. For the LRP-$\alpha\beta$ rule, the parameters $\alpha$ and $\beta$ are subject to the conservation constraint $\alpha = \beta + 1$, and we set default thresholds $\alpha = 1$, $\beta = 0$ to construct a relevance score.

## 4 Experiments

In this section, we evaluate our classification model based on real-world power system datasets. We first introduce the experimental setting. Then experimental results are presented in two parts: comparison results of classification accuracy and illustration of the related feature effects relative to the sample case.

### 4.1 Experimental setup

#### 4.1.1 Dataset

We use the standard IEEE bus test data (Zimmerman et al., 2011), including IEEE 14-bus, IEEE 30-bus, IEEE 39-bus, and IEEE 118-bus. The dataset statistics are summarized in Table 1. To model the load uncertainty, we multiply a random factor drawn uniformly over the interval $[0.9, 1.1]$ to a load of every bus. In this study, we consider $N-1$ and $N-2$ contingencies as the random initial failures. We split the data samples into training set, validation set, and test set.

1. The IEEE 14-bus test case represents a simple approximation of the American Electric Power System as of February 1962. It has 14 buses, 5 generators, 11 loads, and 20 branches.

2. The IEEE 30-bus test case represents a portion of the American Electric Power System (in the U.S. Midwest) as of December 1961. This test case consists of 15 buses, 2 generators, 3 synchronous condensers, and 41 branches.

3. The IEEE 39-bus test system is well known as a 10-machine New England Power System. It contains 39 buses and 46 branches.

4. The IEEE 118-bus power system represents a simple approximation of the American Electric Power System (in the U.S. Midwest) as of December 1962. It contains 118 buses and 186 branches. Fig. 5 shows that IEEE 118 has seven pairs of parallel lines.

#### 4.1.2 Parameter settings

To improve the accuracy of the classification results, it is necessary to explore the best parameters before training the GCN. The sizes of the graph convolutional layers are 128, 64, and 32. All activation functions of the graph convolutional layers are rectified linear units (ReLU). To alleviate overfitting, the graph convolutional layers are followed by a dropout layer with a probability of 0.25. Both the size of the convolutional filters and the probability of a dropout layer are the optimal values found by many experiments in a case study. Categorical cross-entropy is used as the loss function. We train all models using the Adam optimizer with a learning rate of 0.005 with 200 epochs and a batch size of 32. To make a fair comparison to our method, we use the same network architectures, batch-normalization, and global max-pooling. We run experiments for a different Chebyshev filter size ($K = 4$) and report the results in Table 2.

To evaluate our method, we conduct experiments on graph classification tasks. To produce less biased evaluation results, we perform 10-fold cross-validation on the training set. We use the average accuracy across 10-fold testing results with variances.

#### 4.1.3 Baselines

We apply our method to several baseline models, including GCN (Knyazev et al., 2018), the ChebNet spectral convolutional graph (ChebConv) (Defferrard et al., 2016), and UNET (Gao and Ji, 2019). Additionally, to make sure that our method is a good and capable method for capturing the power system topology and improving accuracy, the basic adjacency matrix (original ADJ) and weighted ADJ (W-ADJ) are selected for comparison with power-weighted ADJ (our method).

### 4.2 Experimental results

In this subsection, we explain the classification accuracy results and illustrate the feature effects related to the sample case. To clearly interpret the model, we adjust the MGCN model to be a type

**Table 1 Dataset statistics**

| Dataset | Number of nodes | Number of edges | Number of classes | Average number of nodes | Average number of edges | Number of samples | | |
|---|---|---|---|---|---|---|---|---|
| | | | | | | Training set | Validation set | Test set |
| IEEE 14 | 14 | 20 | 3 | 20 | 36.94 | 10 125 | 3375 | 1500 |
| IEEE 30 | 30 | 41 | 3 | 39.03 | 90.85 | 10 004 | 3335 | 1483 |
| IEEE 39 | 39 | 46 | 3 | 44.02 | 74.45 | 6321 | 2108 | 937 |
| IEEE 118 | 118 | 186 | 3 | 184 | 572.34 | 6599 | 2200 | 978 |

**Table 2 Accuracy of different models in the IEEE test system**

| Topology | Accuracy (%) | | | | | |
|---|---|---|---|---|---|---|
| | IEEE 14 | | | IEEE 30 | | |
| | Original ADJ | W-ADJ | PW-ADJ | Original ADJ | W-ADJ | PW-ADJ |
| GCN | 64.20 (±1.1) | 75.58 (±1.0) | 75.98 (±1.2) | 59.57 (±1.7) | 63.31 (±1.3) | 62.71 (±1.5) |
| ChebConv | 82.23 (±1.2) | 81.49 (±0.5) | 81.76 (±0.5) | 68.01 (±1.3) | 67.46 (±1.3) | 67.38 (±0.9) |
| GCN ($K$=4) | 80.31 (±1.6) | 79.81 (±1.5) | 80.81 (±1.1) | 67.93 (±1.3) | 68.57 (±2.0) | 68.32 (±1.1) |
| MGCN | 73.21 (±7.9) | 79.76 (±2.5) | 79.59 (±2.1) | 64.63 (±1.5) | 64.74 (±1.2) | 65.15 (±1.0) |
| MGCN-ChebConv | 84.06 (±3.0) | **84.12 (±1.9)** | 82.51 (±1.1) | **69.10 (±1.3)** | 68.81 (±1.5) | 68.41 (±0.9) |
| MGCN ($K$=4) | 81.16 (±0.8) | 80.77 (±5.0) | 81.70 (±1.3) | 68.67 (±1.0) | 68.95 (±1.0) | 68.50 (±1.1) |
| UNET | 66.90 (±2.0) | 71.43 (±2.2) | 69.56 (±2.5) | 56.35 (±1.5) | 57.79 (±2.7) | 56.83 (±3.7) |
| Topology | Accuracy (%) | | | | | |
| | IEEE 39 | | | IEEE 118 | | |
| | Original ADJ | W-ADJ | PW-ADJ | Original ADJ | W-ADJ | PW-ADJ |
| GCN | 80.13 (±2.0) | 84.42 (±3.5) | 91.08 (±1.1) | 83.65 (±1.8) | 84.53 (±3.9) | 89.58 (±1.0) |
| ChebConv | 86.28 (±1.1) | 86.88 (±1.7) | 94.63 (±1.5) | 91.14 (±1.2) | 90.91 (±0.9) | 92.49 (±0.6) |
| GCN ($K$=4) | 93.49 (±0.7) | 93.44 (±1.3) | 94.09 (±1.2) | 91.69 (±1.2) | 92.40 (±0.8) | 94.01 (±0.8) |
| MGCN | 90.71 (±4.7) | 89.01 (±6.4) | 95.44 (±2.4) | 89.64 (±0.8) | 88.14 (±1.4) | 88.90 (±1.1) |
| MGCN-ChebConv | 95.84 (±0.8) | 95.26 (±1.0) | 96.61 (±0.7) | 93.33 (±0.7) | 92.95 (±0.7) | 93.17 (±1.0) |
| MGCN ($K$=4) | 95.04 (±3.3) | 95.90 (±2.5) | **97.03 (±1.1)** | 93.89 (±0.3) | 94.07 (±0.6) | **94.21 (±0.6)** |
| UNET | 80.34 (±3.2) | 82.24 (±3.9) | 86.00 (±4.3) | 78.59 (±2.3) | 78.41 (±6.4) | 82.77 (±5.8) |

The best results are in bold. $K$ is a filter scale in graph convolution. ADJ: adjacency matrix. W-ADJ and PW-ADJ denote weighted ADJ and power-weighted ADJ, respectively. The GCN and UNET models use only a single edge. The other models use both edges, where the second edge is learned based on node features

of single-edge graph. LRP is used to explain the rationale behind the component outage classification. The relevance score is the contribution of the input feature.

#### 4.2.1 Model comparison

Table 2 demonstrates the results of the MGCN model with different topologies and other baseline models based on these four datasets. We divide the model comparison into two categories: structural comparison and model comparison.

Structural comparison presents the effect on the graph convolutional model considering spatial information. IEEE 14 and IEEE 30 show that the change of topology does not significantly affect the model accuracy, whereas the results of IEEE 39 and IEEE 118 datasets show that PW-ADJ can capture critical information and dramatically increase the model accuracy. Because of the sparse topology, it is difficult to identify the edge importance of the power system in depth when considering only the graph structure. As expected, spatial information contributes to learning through the topology.

Model comparison shows that the accuracy of our model is higher than that of GCN and UNET. Although the accuracies from IEEE 14 and IEEE 30 are not quite good, MGCN still has higher accuracy than others. Through observation and discussion with an expert, we find that because the protection relay in IEEE 14 and IEEE 30 is not the actual data, it affects the accuracy. In addition, the component outage of the target class level is quite similar; therefore, it is difficult for the model to classify this situation clearly. To observe the MGCN

training process, Fig. 7 shows the changing trend of the loss function with the increase in the number of iterations of the IEEE 39 dataset. IEEE 118 shows that the MGCN model is more suitable for classifying the parallel lines than the GCN model. The accuracy of MGCN increases by $5\%-10\%$ compared with that of GCN. Furthermore, we find that the multi-graph with a larger $K$ obtains better results than the MGCN model. However, for a larger $K$, the model complexity becomes excessive because of the quadratic growth in the number of parameters, and the performance would degrade.

### 4.2.2 Interpretation of MGCN

Based on the accuracy results shown in Table 2, we select IEEE 39 and IEEE 118 samples as case studies. Fig. 8 presents the relevance score of each input feature using our model for the IEEE 39 dataset. The main idea of this interpretation is to identify the most/least relevant feature inputs that contribute to the MGCN model. We can see that the relevance scores of both protection relay and branch flow are positively correlated, whereas the score for load is negatively correlated. A protection relay is a relay device designed for tripping a circuit breaker when a fault is detected. We find that this relay device will act when branch flow (power flow) fluctuates abnormally, and will generate a command to trip a circuit breaker, whereas the load does not have a direct action relationship to a relay. Two situations from the IEEE 39 dataset are considered. In the first situation, after triggering branches L16 and L44, the class is predicted as a medium-level component outage by the model (Fig. 9). In the second situation, after L9 and L44 are triggered, the class is predicted as a high-level component outage by the model (Fig. 10). We can observe that the high relevance scores occur around the initial failure area (Figs. 9 and 10). For both situations, two branches initially fail, in which L44 is the common one, and we find that L14 (6–31), L26 (16–17), and L30 (17–18) are affected.

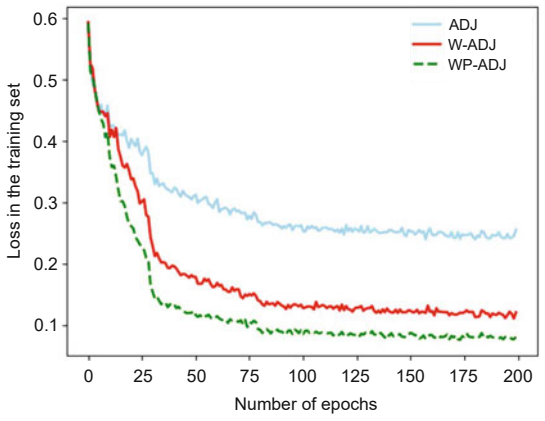


**Fig. 7 The curve of loss in the IEEE 39 test system using the MGCN model**

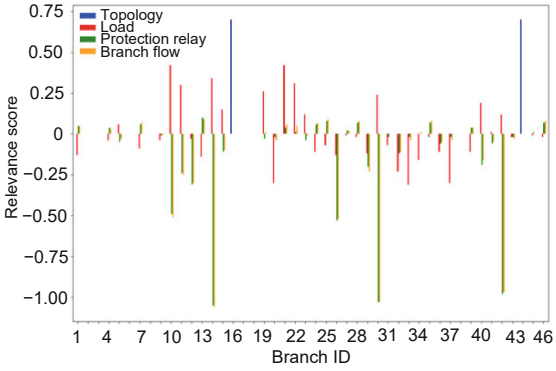


**Fig. 8 Relevance score for each input of the MGCN model that is triggered on the initial failures of L16 and L44 (IEEE 39). References to color refer to the online version of this figure**

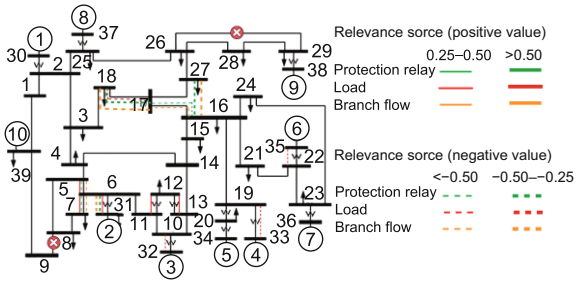


**Fig. 9 Topological graph representing a part of IEEE 39 after L16 and L44 are triggered. The target class is predicted as a medium-level component outage. References to color refer to the online version of this figure**

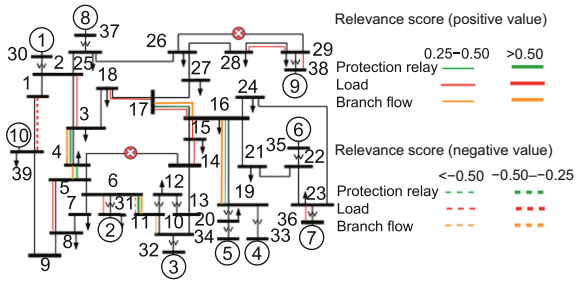


**Fig. 10 Topological graph representing a part of IEEE 39 after L9 and L44 are triggered. The target class is predicted as a high-level component outage. References to color refer to the online version of this figure**

Fig. 11 shows that for the IEEE 118 dataset, after L31 (19–20) fails, the branch flow and protection relay transfer reaction to the entire system, not just the failure area. We find that the locations of the branch flow and protection relay have an effect that occurs around the node that connects to the generator. Additionally, several load values of the system change in the same direction with a high positive relevance score, whereas the power flow of each branch in the power system is not affected in this situation. We also find that the pair of bus nodes that have parallel branches does not have a direct effect on this situation.

## 5 Discussion

In this paper, we propose a novel deep learning based classification model called MGCN, which applies a multi-graph convolutional network to classify the vulnerability effect in cascading failures. Compared with various previous methods, we convert the graph to a line graph to better capture the spatial correlation of the power system and apply the newly proposed MGCN model to classify the component outage and obtain the best classification results on four real-world datasets. In all our experiments, we notice that using more global filters (with a larger $K$) is important. Moreover, the idea of using weighted line graphs can be applied to any given power system topology. We find that the MGCN model can capture both single lines and parallel lines in the power system and increase the accuracy of the classification.

The description of the feature's relevance to the case, derived from calculating the research results, can help users understand the results of the experiments, but cannot be used to adjust the system to improve its learning ability. In the future, we aim to improve the model performance by adding bus node information and applying the model to real-time data. Additionally, we plan to adjust the model using the knowledge given by experts to increase the classification accuracy. There have also been encouraging results in recent studies using chaotic signals to assist energy transport in electrical networks (León-Montiel et al., 2015), using a decentralized strategy

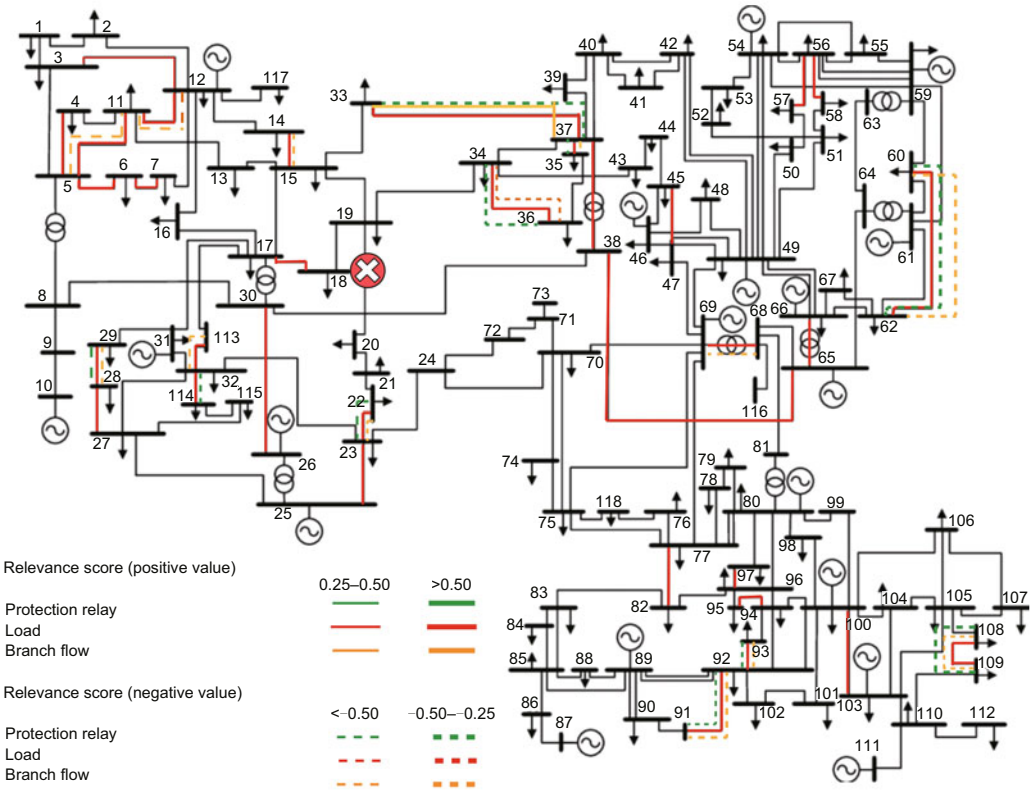


**Fig. 11 Topological graph representing a part of IEEE 118 after L31 is triggered. The target class is predicted as a low-level component outage. References to color refer to the online version of this figure**

to minimize issues in electrical energy distribution in a network (Li Q et al., 2021), and using small chaos control signals to guide the behavior of an electrical system (Bucolo et al., 2021). We think that in future work, we can use these techniques to supplement our approach in reducing power system vulnerabilities.

## 6 Conclusions

In this paper, we have provided an MGCN model for classifying the power system's vulnerability levels in cascading failures. First, we converted the graph to a line graph and constructed a new method to capture the power system topology. Then, we proposed a way to learn new edges in a graph jointly with a graph classification model. Our results showed that the learned edges provided a significant accuracy gain. We also provided an LRP algorithm to uncover the reasons for classifying the cascading failure cases. Case studies on the IEEE 39 and IEEE 118 test systems validated the superiority of the method: (1) Our new weight topology improved the prediction accuracy based on the MGCN model; (2) The MGCN model had a higher efficiency in detecting the component outage events caused by cascading failures; (3) The prediction results of the MGCN model are interpretable, enabling the user to check the logic of the model and uncover the factors that cause the cascading failures. Overall, the proposed method enables an efficient and interpretable analysis of the vulnerabilities of a system in the event of a cascading failure and can contribute to the reliable operation of a power system.

### Contributors

Supaporn LONAPALAWONG designed the study and addressed the problems. Changsheng CHEN processed the data. Supaporn LONAPALAWONG drafted the paper. Changsheng CHEN helped with the technical information. Wei CHEN contributed to material and computing resources, and supervised the study. Can WANG helped organize the paper. Supaporn LONAPALAWONG and Changsheng CHEN revised and finalized the paper.

### Compliance with ethics guidelines

Supaporn LONAPALAWONG, Changsheng CHEN, Can WANG, and Wei CHEN declare that they have no conflict of interest.

### References

Bach S, Binder A, Montavon G, et al., 2015. On pixel-wise explanations for non-linear classifier decisions by layer-wise relevance propagation. *PLoS ONE*, 10(7):e0130140. https://doi.org/10.1371/journal.pone.0130140

Bandyopadhyay S, Biswas A, Murty MN, et al., 2019. Beyond node embedding: a direct unsupervised edge representation framework for homogeneous networks. https://doi.org/10.48550/arXiv.1912.05140

Bolz V, Rueß J, Zell A, 2019. Power flow approximation based on graph convolutional networks. Proc 18th IEEE Int Conf on Machine Learning and Applications, p.1679-1686. https://doi.org/10.1109/ICMLA.2019.00274

Bruna J, Zaremba W, Szlam A, et al., 2014. Spectral networks and locally connected networks on graphs. Proc 2nd Int Conf on Learning Representations, p.1-14.

Bucolo M, Buscarino A, Famoso C, et al., 2021. Chaos addresses energy in networks of electrical oscillators. *IEEE Access*, 9:153258-153265. https://doi.org/10.1109/ACCESS.2021.3127319

Chen G, Dong ZY, Hill DJ, et al., 2010. Attack structural vulnerability of power grids: a hybrid approach based on complex networks. *Phys A Stat Mech Appl*, 389(3): 595-603. https://doi.org/10.1016/j.physa.2009.09.039

Chen KJ, Hu J, Zhang Y, et al., 2020. Fault location in power distribution systems via deep graph convolutional networks. *IEEE J Sel Area Commun*, 38(1):119-131. https://doi.org/10.1109/JSAC.2019.2951964

Defferrard M, Bresson X, Vandergheynst P, 2016. Convolutional neural networks on graphs with fast localized spectral filtering. Proc 30th Int Conf on Neural Information Processing Systems, p.3844-3852.

di Muro MA, Valdez LD, Rêgo HHA, et al., 2017. Cascading failures in interdependent networks with multiple supply-demand links and functionality thresholds. *Sci Rep*, 7(1):15059. https://doi.org/10.1038/s41598-017-14384-y

Eppstein MJ, Hines PDH, 2012. A "random chemistry" algorithm for identifying collections of multiple contingencies that initiate cascading failure. *IEEE Trans Power Syst*, 27(3):1698-1705. https://doi.org/10.1109/TPWRS.2012.2183624

Fang JY, Wu JJ, Zheng ZB, et al., 2021. Revealing structural and functional vulnerability of power grids to cascading failures. *IEEE J Emerg Sel Top Circ Syst*, 11(1):133-143. https://doi.org/10.1109/JETCAS.2020.3033066

Gambuzza LV, Buscarino A, Fortuna L, et al., 2017. Analysis of dynamical robustness to noise in power grids. *IEEE J Emerg Sel Top Circ Syst*, 7(3):413-421. https://doi.org/10.1109/JETCAS.2017.2649598

Gao HY, Ji SW, 2019. Graph U-Nets. Proc 36th Int Conf on Machine Learning, p.2083-2092.

Ge LJ, Liao WL, Wang SX, et al., 2020. Modeling daily load profiles of distribution network for scenario generation using flow-based generative network. *IEEE Access*, 8:77587-77597. https://doi.org/10.1109/ACCESS.2020.2989350

Henaff M, Bruna J, LeCun Y, 2015. Deep convolutional networks on graph-structured data. https://arxiv.org/abs/1506.05163

Hu JL, Li TH, Dong SB, 2020. GCN-LRP explanation: exploring latent attention of graph convolutional networks. Proc Int Joint Conf on Neural Networks, p.1-8. https://doi.org/10.1109/IJCNN48605.2020.9207639

Kim C, Kim K, Balaprakash P, et al., 2019. Graph convolutional neural networks for optimal load shedding under line contingency. Proc IEEE Power & Energy Society General Meeting, p.1-5. https://doi.org/10.1109/PESGM40551.2019.8973468

Kipf TN, Welling M, 2017. Semi-supervised classification with graph convolutional networks. Proc 5th Int Conf on Learning Representations, p.1-14.

Knyazev B, Lin X, Amer MR, et al., 2018. Spectral multigraph networks for discovering and fusing relationships in molecules. https://arxiv.org/abs/1811.09595

Kohlbrenner M, Bauer A, Nakajima S, et al., 2020. Towards best practice in explaining neural network decisions with LRP. Proc Int Joint Conf on Neural Networks, p.1-7. https://doi.org/10.1109/IJCNN48605.2020.9206975

León-Montiel RD, Quiroz-Juárez MA, Quintero-Torres R, et al., 2015. Noise-assisted energy transport in electrical oscillator networks with off-diagonal dynamical disorder. *Sci Rep*, 5:17339. https://doi.org/10.1038/srep17339

Li Q, Liao YX, Wu KM, et al., 2021. Parallel and distributed optimization method with constraint decomposition for energy management of microgrids. *IEEE Trans Smart Grid*, 12(6):4627-4640. https://doi.org/10.1109/TSG.2021.3097047

Li X, Qi ZT, 2021. Impact of cascading failure based on line vulnerability index on power grids. *Energy Syst*, early access. https://doi.org/10.1007/s12667-021-00435-x

Liao WL, Yang DC, Wang YS, et al., 2021. Fault diagnosis of power transformers using graph convolutional network. *CSEE J Power Energy Syst*, 7(2):241-249. https://doi.org/10.17775/CSEEJPES.2020.04120

Liu YX, Zhang N, Wu D, et al., 2021. Searching for critical power system cascading failures with graph convolutional network. *IEEE Trans Contr Netw Syst*, 8(3): 1304-1313. https://doi.org/10.1109/TCNS.2021.3063333

Lonapalawong S, Yan JZ, Li JY, et al., 2022. Reducing power grid cascading failure propagation by minimizing algebraic connectivity in edge addition. *Front Inform Technol Electron Eng*, 23(3):382-397. https://doi.org /10.1631/FITEE.2000596

Luo B, Wang HT, Liu HQ, et al., 2019. Early fault detection of machine tools based on deep learning and dynamic identification. *IEEE Trans Ind Electron*, 66(1):509-518. https://doi.org/10.1109/TIE.2018.2807414

Mei SW, He F, Zhang XM, et al., 2009. An improved OPA model and blackout risk assessment. *IEEE Trans Power Syst*, 24(2):814-823. https://doi.org/10.1109/TPWRS.2009.2016521

Montavon G, Binder A, Lapuschkin S, et al., 2019. Layer-wise relevance propagation: an overview. In: Samek W, Montavon G, Vedaldi A, et al. (Eds.), Explainable AI: Interpreting, Explaining and Visualizing Deep Learning. Springer, Cham, p.193-209. https://doi.org/10.1007/978-3-030-28954-6_10

Owerko D, Gama F, Ribeiro A, 2018. Predicting power outages using graph neural networks. Proc IEEE Global Conf on Signal and Information Processing, p.743-747. https://doi.org/10.1109/GlobalSIP.2018.8646486

Pizzuti C, Socievole A, van Mieghem P, 2020. Comparative network robustness evaluation of link attacks. Proc Int Conf on Complex Networks and Their Applications, p.735-746. https://doi.org/10.1007/978-3-030-36687-2_61

Ren WD, Wu JJ, Zhang X, et al., 2018. A stochastic model of cascading failure dynamics in communication networks. *IEEE Trans Circ Syst II Expr Briefs*, 65(5):632-636. https://doi.org/10.1109/TCSII.2018.2822049

Schnake T, Eberle O, Lederer J, et al., 2020. Higher-order explanations of graph neural networks via relevant walks. https://arxiv.org/abs/2006.03589v3

Schneider CM, Moreira AA, Andrade JSJr, et al., 2011. Mitigation of malicious attacks on networks. *Proc Natl Acad Sci USA*, 108(10):3838-3841. https://doi.org/10.1073/pnas.1009440108

Song JJ, Cotilla-Sanchez E, Ghanavati G, et al., 2016. Dynamic modeling of cascading failure in power systems. *IEEE Trans Power Syst*, 31(3):2085-2095. https://doi.org/10.1109/TPWRS.2015.2439237

Springenberg JT, Dosovitskiy A, Brox T, et al., 2015. Striving for simplicity: the all convolutional net. Proc 3rd Int Conf on Learning Representations, p.1-14.

Tong HJ, Qiu RC, Zhang DX, et al., 2021. Detection and classification of transmission line transient faults based on graph convolutional neural network. *CSEE J Power Energy Syst*, 7(3):456-471. https://doi.org/10.17775/CSEEJPES.2020.04970

Wu J, Barahona M, Tan YJ, et al., 2011. Spectral measure of structural robustness in complex networks. *IEEE Trans Syst Man Cybern Part A Syst Humans*, 41(6):1244-1252. https://doi.org/10.1109/TSMCA.2011.2116117

Ying R, He RN, Chen KF, et al., 2018. Graph convolutional neural networks for web-scale recommender systems. Proc 24th ACM SIGKDD Int Conf on Knowledge Discovery & Data Mining, p.974-983. https://doi.org/10.1145/3219819.3219890

Zeiler MD, Fergus R, 2014. Visualizing and understanding convolutional networks. Proc 13th European Conf on Computer Vision, p.818-833.

Zhang X, Tse CK, 2015. Assessment of robustness of power systems from a network perspective. *IEEE J Emerg Sel Top Circ Syst*, 5(3):456-464. https://doi.org/10.1109/JETCAS.2015.2462152

Zhang X, Zhan CJ, Tse CK, 2017. Modeling the dynamics of cascading failures in power systems. *IEEE J Emerg Sel Top Circ Syst*, 7(2):192-204. https://doi.org/10.1109/JETCAS.2017.2671354

Zhou BL, Khosla A, Lapedriza À, et al., 2016. Learning deep features for discriminative localization. Proc IEEE Conf on Computer Vision and Pattern Recognition, p.2921-2929. https://doi.org/10.1109/CVPR.2016.319

Zhu YH, Yan J, Sun Y, et al., 2014. Revealing cascading failure vulnerability in power grids using risk-graph. *IEEE Trans Parall Distrib Syst*, 25(12):3274-3284. https://doi.org/10.1109/TPDS.2013.2295814

Zimmerman RD, Murillo-Sánchez CE, Thomas RJ, 2011. MATPOWER: steady-state operations, planning, and analysis tools for power systems research and education. *IEEE Trans Power Syst*, 26(1):12-19. https://doi.org/10.1109/TPWRS.2010.2051168